Available online at www.sciencedirect.com
SCIENCE DIRECT
Biochemical Pharmacology 70 (2005) 1579–1592
Biochemical Pharmacology
www.elsevier.com/locate/biochempharm

The ethyl pyruvate analogues, diethyl oxaloproprionate, 2-acetamidoacrylate, and methyl-2-acetamidoacrylate, exhibit anti-inflammatory properties in vivo and/or in vitro

Penny L. Sappington [a], Ruy J. Cruz Jr. [a], Tomoyuki Harada [a], Runkuan Yang [a], Yusheng Han [a], Joshua A. Englert [a], Alfred A. Ajami [b], Meaghan E. Killeen [a], Russell L. Delude [a,c], Mitchell P. Fink [a,d,*]

[a] *Department of Critical Care Medicine, University of Pittsburgh School of Medicine, 616 Scaife Hall, 3550 Terrace Street, Pittsburgh, PA 15261, USA*
[b] *Xanthus Life Sciences, Inc., Cambridge, MA 02139, USA*
[c] *Department of Pathology, University of Pittsburgh School of Medicine, Pittsburgh, PA 15261, USA*
[d] *Department of Surgery, University of Pittsburgh School of Medicine, Pittsburgh, PA 15261, USA*

Received 1 June 2005; accepted 25 August 2005

Abstract

Ethyl pyruvate (EP) is a simple aliphatic ester derived from the endogenous metabolite, pyruvic acid. EP has been shown to decrease the expression of various pro-inflammatory mediators, including nitric oxide ($NO^{\bullet}$), tumor necrosis factor (TNF), cyclooxygenase-2, and interleukin (IL)-6, in a variety of in vitro and in vivo model systems. In an effort to better understand the chemical features that might explain the anti-inflammatory properties of EP, we screened 15 commercially available compounds for cytoprotective or anti-inflammatory effects using two in vitro assay systems: TNF and $NO^{\bullet}$ production by lipopolysaccharide (LPS)-stimulated RAW 264.7 murine macrophage-like cells and changes in the permeability of Caco-2 human enterocyte-like monolayers stimulated with a cocktail of pro-inflammatory cytokines called cytomix (1000 U/ml IFN-γ plus 10 ng/ml TNF-α plus 1 ng/ml IL-1β). Two compounds, namely diethyl oxaloproprionate (DEOP) and 2-acetamidoacrylate (2AA), demonstrated consistent anti-inflammatory or cytoprotective pharmacological properties in this screening process. Treatment of mice with either of these compounds ameliorated LPS-induced ileal mucosal hyperpermeability to the fluorescent probe, fluorescein isothiocyanate-labeled dextran (average molecular mass 4 kDa), and bacterial translocation to mesenteric lymph nodes. Treatment with either of these compounds also improved survival in mice challenged with a lethal dose of LPS. Finally, in a study that compared 2AA to its methyl ester, we showed that methyl-2-acetamidoacrylate is at least 100-fold more potent than the parent carboxylate as an inhibitor of LPS-induced $NO^{\bullet}$ production by RAW 264.7 cells. Collectively, these data are consistent with the view that anti-inflammatory activity is demonstrable for a number of compounds that either incorporate an olefinic linkage conjugated to a carbonyl moiety or are capable of undergoing tautomeric rearrangement to form such a structure. Moreover, our findings suggest that esters with these general characteristics, perhaps because of their greater lipophilicity or electrophilicity, are more potent anti-inflammatory agents than are the parent carboxylates.

Ethyl pyruvate (EP) is a simple aliphatic ester derived from the endogenous metabolite, pyruvic acid. In previous studies performed by our laboratory and others, EP has been shown to ameliorate intestinal, renal or hepatic injury when it is used as a therapeutic agent to treat rodents subjected to mesenteric ischemia and reperfusion [1,2], coronary ischemia and reperfusion [3], hemorrhagic shock [4,5], endotoxemia [6,7], or polymicrobial bacterial sepsis [6,8,9]. Treatment with EP also ameliorates organ dysfunction in murine models of acute pancreatitis [10], alcoholic hepatitis [11], and biliary obstruction [12]. In many of these models of acute critical illness, treatment with EP down-regulates the expression of various pro-inflammatory genes, including inducible nitric oxide synthase (iNOS), tumor necrosis factor (TNF), cyclooxygenase-2, and interleukin (IL)-6 [2,5,10,11]. Similarly, EP inhibits IL-6 and iNOS expression, nitric oxide ($NO^{\bullet}$) production, and/or secretion of the

* Corresponding author. Tel.: +1 412 647 6965; fax: +1 412 647 5258.
E-mail address: finkmp@ccm.upmc.edu (M.P. Fink).

0006-2952/$ – see front matter © 2005 Elsevier Inc. All rights reserved.
doi:10.1016/j.bcp.2005.08.015

pro-inflammatory protein, HGMB1, by immunostimulated Caco-2 human enterocyte-like cells or lipopolysaccharide (LPS)-stimulated RAW 264.7 murine macrophage-like cells [6,13–15]. These latter findings support the view that EP has activity as an anti-inflammatory agent.

The molecular mechanisms underlying the anti-inflammatory effects of EP remain to be elucidated. In an effort to better understand the chemical features that might explain the anti-inflammatory properties of EP, we screened 15 commercially available compounds for cytoprotective or anti-inflammatory effects using two in vitro assay systems: TNF and $NO^{\bullet}$ production by LPS-stimulated RAW 264.7 murine macrophage-like cells and changes in the permeability of Caco-2 human enterocyte-like monolayers stimulated with a cocktail of pro-inflammatory cytokines called cytomix (1000 U/ml IFN-γ plus 10 ng/ml TNF-α plus 1 ng/ml IL-1β). Two compounds, namely diethyl oxaloproprionate (DEOP) and 2-acetamidoacrylate (2AA), demonstrated consistent anti-inflammatory or cytoprotective pharmacological properties in this screening process. The salutary effects of these compounds were verified in a series of more detailed studies, using both in vitro assay systems as well as a murine model of LPS-induced organ injury and lethality. Finally, in a study that compared 2AA to its methyl ester, we showed that methyl-2-acetamidoacrylate is at least 100-fold more potent than the parent carboxylate (EP or 2AA) as an inhibitor of LPS-induced $NO^{\bullet}$ production by RAW 264.7 cells.

1. Methods

1.1. Animals

Male C57BL/6J mice (Jackson Laboratories, Bar Harbor, ME) weighing 20–25 g were used in this study. All animals were maintained at the University of Pittsburgh Animal Research Center with a 12-h light:12-h dark cycle and free access to standard laboratory chow and water. Animals were not fasted prior to the experiments. The research protocol complied with the regulations regarding animal care as published by the National Institutes of Health and was approved by the Institutional Animal Use and Care Committee of the University of Pittsburgh Medical School.

1.2. Materials

All chemicals were purchased from Sigma–Aldrich Chemical Co. (St. Louis, MO) unless otherwise noted. DMEM and PBS were from BioWhittaker (Walkersville, MD). FBS was from Hyclone (Logan, UT). IFN-γ, TNF, and IL-1β were obtained from Pierce-Endogen (Rockford, IN). Caco-2 human intestinal epithelial cells and BALB/c murine macrophage-like RAW 264.7 cells were obtained from the American Type Culture Collection (Manassas, VA).

1.3. Cell culture

For the screening assays (Figs. 1 and 2), RAW 264.7 cells, obtained from the American Type Culture Collection (ATCC TIB-71), were cultured in RPMI medium 1640 (Life Technologies, Grand Island, NY) supplemented with 10% heat-inactivated FBS (Gemini Biological Products, Calabasas, CA), 2 mM glutamine (25030-149; GIBCO/BRL), and antibiotic–antimycotic mix (15240-062; GIBCO/BRL) in a humidified incubator with 5% CO_2 and 95% air. Cells were removed mechanically and resuspended in serum-free Opti-MEM I medium (Life Technologies) to perform experiments at 75% confluence.

For the more detailed concentration–response studies (Figs. 11 and 12), RAW 264.7 cells were grown in Dulbecco's minimum essential medium (DMEM) supplemented with 10% heat-inactivated FBS, penicillin G (100 U/ml), streptomycin (100 μg/ml), pyruvate (2 mM), and nonessential amino acids. The cells were plated (300,000 cells per well) in 1 ml of medium in 24-well dishes, and incubated overnight at 37 °C. The following day, the medium was changed to DMEM supplemented

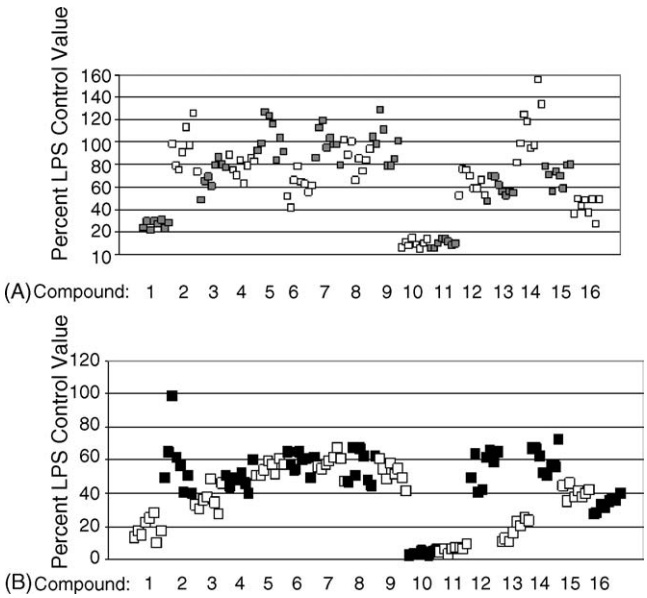

Fig. 1. Effect of compounds 1–16 on LPS-induced TNF secretion (Panel A) and LPS-induced $NO^{\bullet}$ production (Panel B) by RAW 264.7 cells. The names and structures of the compounds are depicted in Table 1. Each compound was tested under eight different conditions ($n = 1$ per condition). For each compound, the results for each condition are shown in the figure in the same order as the conditions are shown in Table 2. $NO^{\bullet}$ production was assayed by measuring nitrite concentrations in culture supernatants. Results are presented as percent of control TNF or nitrite concentration (for cells incubated for the same period in presence of the same concentration of LPS in the absence of a test compound). The control values for TNF were as follows: LPS 0.01 μg/ml for 12 h, 66 nM; LPS 0.01 μg/ml for 24 h, 99 nM; LPS 1 μg/ml for 12 h, 91 nM; LPS 1 μg/ml for 24 h, 100 nM. The control values for nitrite were as follows: LPS 0.01 μg/ml for 12 h, 10 μM; LPS 0.01 μg/ml for 24 h, 12 μM; LPS 1 μg/ml for 12 h, 22 μM; LPS 1 μg/ml for 24 h, 26 μM. The shading of alternating groups of symbols (one cluster per compound) is intended only to enhance clarity.

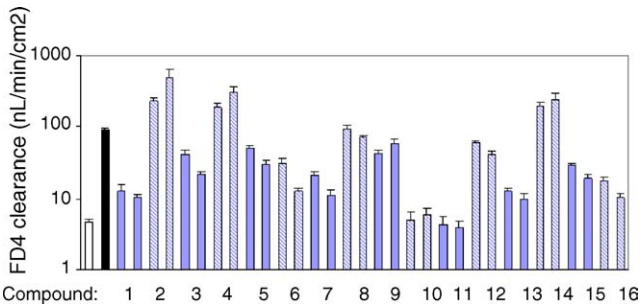

Fig. 2. Effect of compounds 1–16 on the permeability of Caco-2 human enterocyte-like monolayers incubated with cytomix. The names and structures of the compounds are depicted in Table 1. Each compound was tested at 1 and 5 mM final concentration ($n = 6$ per condition). The open bar represents the mean (±S.E.M.) clearance of FD4 for cells incubated for 48 h in the absence of cytomix ($n = 6$). The black bar represents the mean (±S.E.M.) clearance of FD4 for cells incubated for 48 h in the presence of cytomix ($n = 5$). The gray or cross-hatched shading of alternating groups of symbols (one cluster per compound) is intended only to enhance clarity. The data were not evaluated statistically.

with 0.25% heat-inactivated FBS and the cells were stimulated in the presence or absence of LPS and the test compounds.

Caco-2 human intestinal epithelial cells were routinely maintained on collagen-1 coated Biocoat tissue culture dishes (Becton-Dickonson, Bedform, MA) at 37 °C in a 5% CO_2 humidified atmosphere in DMEM supplemented with 10% FBS, penicillin G (100 U/ml), streptomycin (100 μg/ml), pyruvate (2 mM), L-glutamine (4 mM), and nonessential amino acids.

1.4. Monolayer permeability assays

Caco-2 human enterocyte-like cells (10^5 cells/well) were plated on permeable filters in 12-well Transwell bicameral chambers (COSTAR, Corning, NY) and fed biweekly. Permeability studies were carried out using confluent monolayers between 21 and 28 day after seeding. The permeability probe was FITC-labeled dextran (4000 Da; FD4). A sterile stock solution of FD4 (25 mg/ml) was prepared by dissolving the compound in HEPES-buffered DMEM complete medium (pH 6.8) and passing it through a filter (0.45 μm pore size). For permeability studies, the medium was aspirated from the apical and basolateral sides of the Transwell chambers. FD4 solution (200 μl) was added to the apical compartments. The medium on the basolateral side of the Transwell chambers was replaced with 500 μl of control medium, medium with cytomix, or medium with cytomix plus various concentrations of the compounds to be tested. After 48 h of incubation, 30 μl of medium was aspirated from the basolateral compartments for fluorometric determination of FD4 concentration as previously described [16]. The permeability of monolayers was expressed as an average clearance (C), which was calculated as previously described [16].

1.5. Reverse transcriptase-polymerase chain reaction (RT-PCR)

Total RNA was extracted from harvested tissues or RAW cells with chloroform and TRI Reagent (Molecular Research Center, Cincinnati, OH) exactly as directed by the manufacturer. The total RNA was treated with DNA-Free (Ambion, Houston, TX) as instructed by the manufacturer using 10 units of DNase I/10 μg RNA. Two micrograms of total RNA was reverse transcribed in a 40 μl reaction volume containing 0.5 μg of oligo$(dT)_{15}$ (Promega, Madison, WI), 1 mM of each dNTP, 15 U AMV reverse transcriptase (Promega), and 1 U/μl of recombinant RNasin ribonuclease inhibitor (Promega) in 5 mM $MgCl_2$, 10 mM Tris, pH 8.0, 50 mM KCl, and 0.1% Triton X-100. The reaction mixtures were pre-incubated at 21 °C for 10 min prior to DNA synthesis. The RT reactions were carried out for 50 min at 42 °C and were heated to 95 °C for 5 min to terminate the reaction. Reaction mixtures (50 μl) for PCR were assembled using 5 μl of cDNA template, 10 units AdvanTaq Plus DNA Polymerase (Clontech, Palo Alto, CA), 200 μM of each dNTP, 1.5 mM $MgCl_2$ and 1.0 μM of each primer in 1× AdvanTaq Plus PCR buffer. PCR reactions were performed using a Model 480 thermocycler (Perkin-Elmer, Norwalk, CT). Amplification of cDNA for iNOS was carried out by denaturing at 94 °C for 45 s, annealing at 58 °C for 1 min, and polymerizing at 72 °C for 45 s for 20 cycles. This number of PCR cycles was empirically determined to ensure that amplification was in the linear range. After the last cycle of amplification, the samples were incubated in 72 °C for 10 min and then held at 4 °C. The 5′ and 3′ primers for iNOS were CAC CAC AAG GCC ACA TCG GAT T and CCG ACC TGA TGT TGC CAT TGT T, respectively (Invitrogen, Carlsbad, CA); the expected product length was 426 bp. 18S ribosomal RNA was amplified to verify equal loading. For this reaction, the 5′ and 3′ primers were CCC GGG GAG GTA GTG ACG AAA AAT and CGC CCG CTC CCA AGA TCC AAC TAC, respectively; the expected product length was 209 bp. Ten microliters of each PCR reaction were electrophoresed on a 2% agarose gel, scanned at a NucleoVision imaging workstation (NucleoTech, San Mateo, CA), and quantified using GelExpert release 3.5.

1.6. Measurement of $NO^{\bullet}$ production

To obtain the data depicted in Figs. 2 and 9, concentrations of NO_3^- plus NO_2^-, the end products of $NO^{\bullet}$ metabolism, in tissue culture supernatants or plasma were estimated by first reducing NO_3^- to NO_2^-. Cadmium (Cd) filings (0.4–0.7 g/tube; Fluka, Milwaukee, WI) were loaded into 1.5 ml microfuge tubes. The filings were washed twice with 1.0 ml of deionized water, twice with 1.0 ml of 0.1 M HCl, and twice with 1.0 ml of 0.1 M NH_4OH. Ten microliters of 30% $ZnSO_4$ was added to

200 μl of culture supernatant, vortexed, incubated at room temperature for 15 min, and centrifuged at 14,000 × *g* for 5 min. The resulting supernatant was added to a Cd-containing microcentrifuge tube and incubated at room temperature overnight with constant mixing. The samples were transferred to fresh microcentrifuge tubes and centrifuged again. The supernatants were subsequently assayed for NO_2^-, using the Griess assay as previously described [17]. To obtain the data depicted in Fig. 12, NO_2^- concentrations in tissue culture supernatants were assessed using a commercially available assay kit (Oxis International, Portland OR).

1.7. TNF assay

TNF was measured in cell culture supernatants using a commercially available enzyme-linked immunosorbent assay (ELISA) kit from BD Biosciences (San Diego, CA), according to the manufacturer's specifications.

1.8. Nuclear extract preparation

Caco-2 enterocytes were plated at 10^6 cells per well in 6-well dishes for 21 days. The Caco-2 cells were incubated with control medium, medium with cytomix, medium with 1 or 5 mM 2AA or DEOP plus cytomix, or medium with 5 mM EP and cytomix. After stimulation for 4 h, the cells were removed from the incubator and immediately placed on ice. Cells were washed once with PBS then harvested in 1 ml of PBS containing 2% FBS using a rubber policeman. The cells were transferred to a 1.5 ml microfuge tube and centrifuged at 14,000 × *g* for 10 s. The cell pellet was resuspended in 600 μl of buffer I (10 mM KCl, 1.5 mM $MgCl_2$, 0.3 M sucrose, 500 μM PMSF, 1.0 mM sodium orthovanadate, 1 mM DTT, 10 mM Tris, pH 7.8) and incubated for 15 min. Subsequently, 38.3 μl of 10% NP40 was the added and the tubes were vortexed at full speed for 10 s. The nuclei were isolated by centrifugation at 310 × *g* for 3 min and the supernatants were aspirated. The nuclear pellets were gently resuspended in 80 μl of buffer II (500 μM PMSF, 1.0 mM sodium orthovanadate, 1 mM DTT, 420 mM KCl, 1.5 mM $MgCl_2$, 20% glycerol, 10 mM Tris, pH 7.8). Following 15 min incubation, nuclear extracts were cleared by centrifugation at 14,000 × *g* for 10 min. The supernatants were transferred to new tubes, and protein concentration was determined using a commercially available Bradford assay (Bio-Rad Protein Assay, Hercules, CA). Nuclear extracts were frozen at −80 °C.

1.9. Electrophoretic mobility shift assay (EMSA)

The sequence of the double-stranded NF-κB oligonucleotide was as follows: sense, 5′-AGT TGA GGG GAC TTT CCC AGG C-3′; antisense, 3′-TCA ACT CCC CTG AAA GGG TCC G-5′ (Promega). The oligonucleotides were end-labeled with γ-^{32}P ATP (New England Nuclear, Boston, MA) using T4 polynucleotide kinase (Promega). Three micrograms of nuclear protein was incubated with the [^{32}P]-labeled NF-κB probe (1 μl) in 4 μl of 5× band-shift buffer (325 mM NaCl, 5 mM DTT, 0.7 mM EDTA, 40%, v/v, glycerol, 65 mM HEPES, pH 8.0) in the presence of 2 μg of poly(dI-dC) (Boehringer Mannheim, Indianapolis, IN) for 20 min at room temperature. For competition reactions, a 100-fold molar excess of cold oligonucleotide was added simultaneously with labeled probe. Supershift assays were performed by incubating nuclear extracts with 2 μl of anti-p65 and anti-p50 monoclonal antibody (Santa Cruz Biotechnology, Santa Cruz, CA) for 1 h prior to the addition of the radiolabeled probe. The binding reaction mixture was electrophoresed on 4% nondenaturing PAGE gels containing 5% glycerol and 1/4× Tris–borate–EDTA (TBE) buffer. After PAGE, the gels were dried and used to exposed Biomax-5 film (Kodak, Rochester, NY) at −80 °C overnight using an intensifying screen.

1.10. Preparation of whole cell extracts for Western blotting

After washing with ice-cold phosphate-buffered saline, cells were lysed in 1 ml of radioimmunoprecipitation buffer, consisting of 1× phosphate-buffered saline, 1% NP40, 0.5% sodium deoxycholate, 0.1% SDS, 0.1 mg/ml phenylmethylsulfonyl fluoride, 1.0 mM sodium orthovanadate, and 1× mammalian protease inhibitor cocktail (Sigma–Aldrich, catalog no. P8340). The cells were removed from the tissue culture plate and transferred to a 1.5-ml microfuge tube and incubated for 30 min on ice. The lysate was centrifuged at 12,000 × *g* for 5 min at 4 °C. Protein concentrations were quantitated using the Bio-Rad assay.

1.11. Western blotting of whole cell or nuclear extracts

Equal amounts of total protein extract were mixed in 2× Laemmli buffer, boiled for 5 min, and centrifuged for 10 s. Proteins were resolved by electrophoresis on 10% SDS-polyacrylamide gel electrophoresis, transferred to a Hybond-P polyvinylidene difluoride membrane (Amersham Biosciences Inc., Piscataway, NJ), and probed sequentially with antibody. The filter was incubated at 4 °C for 24 h with primary antibody in TBST (10 mM Tris, pH 7.5, 150 mM NaCl, and 0.5% Tween 20). After being washed three times in TBST, immunoblots were exposed for 1 h to the appropriate peroxidase-conjugated secondary antibody. After three washes in TBST, the membrane was impregnated with the enhanced chemiluminescence substrate (Amersham Biosciences Inc.) and used to expose X-ray film. The following antibodies were used: rabbit polyclonal anti-IκBα (Santa Cruz Biotechnology, Inc.) 1:500 dilution, rabbit polyclonal anti-IκBβ (Santa Cruz Biotechnology, Inc.) 1:500 dilution, mouse monoclonal anti-p65 (Santa Cruz Biotechnology, Inc.)

1:200 dilution, rabbit anti-mouse IgG peroxidase conjugate (Sigma–Aldrich) 1: 4000 dilution, goat anti-mouse IgG peroxidase conjugate (Sigma–Aldrich) 1:20,000 dilution.

1.12. Experimental designs for in vivo experiments

In the first of three in vivo experiments, five groups of mice ($N = 5$ each) were studied. All agents were injected intraperitoneally. Mice in the PBS + RLS group (i.e., the negative control group) were injected with 1.0 ml of PBS (pH 7.4), whereas mice in all of the other groups were injected with 1.0 ml of a suspension (0.1 mg/ml) of *Escherichia coli* O111:B4 LPS in PBS. One, 6, and 12 h later, mice in the PBS + RLS and LPS + RLS groups were injected with 0.31 ml (we do not have syringes that are this accurate; should be 0.3 ml) of Ringer's lactate solution (RLS), a balanced salt solution containing 109 mM NaCl, 4.0 mM KCl, 2.7 mM $CaCl_2$, and 28 mM sodium lactate. Mice in the remaining three groups (LPS + EP, LPS + DEOP, and LPS + 2AA) received three injections of the appropriate compound (i.e., EP, DEOP or 2AA). The doses contained 0.34 mmol of the relevant compound dissolved in RLS (volume?) and were administered 1, 6, and 12 h after the injection of LPS. Eighteen hours after injection of LPS or PBS, the mice were anesthetized with sodium pentobarbital (90 mg/kg, i.p.) and ileal mucosal permeability to FD4 was determined using an ex vivo everted gut sac method, as previously described by Yang et al. [5]. The mesenteric lymph node (MLN) complex was excised and bacterial translocation determined, as previously described by Yang et al. [5]. Blood was aspirated from the heart, and the plasma was collected by centrifugation and stored at −80 °C for subsequent determinations of alanine aminotransferase (ALT) and NO_2^- concentrations.

The second experiment was carried out exactly as described above, except that a portion of liver tissue was obtained 18 h after the injection of PBS or LPS. The hepatic tissue was stored frozen at −80 °C until assayed for total glutathione (GSH) content.

The third experiment was a survival study. The groups were the same as described above. Survival was monitored for 7 days.

1.13. ALT assay

Two hundred microliters of blood was obtained by cardiac puncture and placed in a 0.5 ml centrifugation tube on ice. After being allowed to clot, the sample was centrifuged at 5000 × *g* for 3 min. The serum was aspirated and assayed for ALT concentration by the clinical laboratory at the University of Pittsburgh Medical Center.

1.14. Lipid peroxidation assay

The assay for lipid peroxidation was performed as described previously [4]. In brief, after tissue specimens were thawed, 0.4 ml of phosphate buffer (PBS?) was added to 200 mg of tissue. The tissue was homogenized. Trichloroacetic acid (20%, w/v, solution; 1.25 ml) and thiobarbituric acid (0.67%, w/v, solution; 0.50 ml) were added to 0.25 ml of the tissue homogenate. The color of the thiobarbituric acid pigment was developed by incubating the mixture in a boiling water bath for 30 min. After cooling the mixture to room temperature by immersion in tap water, 2 ml of *n*-butanol was added and shaken vigorously. After centrifugation, absorbance of the butanol layer was determined at 535 nm. Samples were run in duplicate and the results were averaged. We used 1,1,3,3-tetraethoxypropane to generate a standard curve. Results were expressed as nanomoles of MDA per gram of tissue.

1.15. Glutathione (GSH) assay

Total glutathione concentration was determined using ThioGlo-1 (Calbiochem, San Diego, CA), a maleimide reagent that produces a highly fluorescent adduct upon its reaction with free thiol groups. Tissue specimens were thawed on ice, 1.5 ml of phosphate buffer (0.05 M, pH 7.4) was added to approximately 100 mg of tissue and sonicated using an Ultrasonic homogenizer (Brinkmann, Westbury, NY). GSH content in samples was estimated as described previously [18] by measuring the immediate increase in fluorescence after the addition of ThioGlo-1 using a Fusion Plate Reader (Packard, Boston, MA) with an excitation wavelength of 335 ± 60 nm and an emission wavelength 535 ± 25 nm. The GSH content of each sample was measured twice and the results were expressed as nanomoles of GSH per gram of tissue ± S.E.M.

1.16. Statistical methods

Results are presented as means ± S.E.M. In general, data were analyzed using analysis of variance (ANOVA) followed by Fisher's protected L.S.D. test. Bacterial translocation data were analyzed using nonparametric methods (Kruskal–Wallis nonparametric ANOVA and Mann–Whitney *U*-test). Differences in survival were assessed using Fisher's exact test. *p*-Values <0.05 were considered significant.

2. Results

2.1. EP, 2AA, and DEOP inhibit $NO^\bullet$ and TNF secretion by LPS-stimulated RAW 264.7 cells

In addition to EP, we screened 15 other compounds for biological activity in three different in vitro assays (LPS-induced TNF secretion by RAW 264.7 cells, LPS-induced $NO^\bullet$ secretion by RAW 264.7 cells, and cytomix-induced hyperpermeability of Caco-2 monolayers). The compounds and their chemical structures are shown in

Table 1. Like EP, compounds 2–4, 6–8, and 11 are ethyl esters of a mono- or dicarboxylic acid. Like EP, compounds 2, 4, 5, 7, 11, and 13–15 are α-keto derivatives of a mono- or dicarboxylic acid. Compound 10 recapitulates the structure of the enol tautomer of EP. Compound 12 is a simple three-carbon sugar that is converted by cells, including enterocytes, into pyruvate and subsequently used as an oxidative substrate [19,20]. Compound 16, an extensively studied cell-permeable scavenger of reactive oxygen species (ROS), was included among the screened compounds because pyruvate is known to scavenge hydrogen peroxide (H_2O_2) and other ROS [21–23], and EP has been shown to inhibit lipid peroxidation in vivo and in vitro [4,15].

We previously reported that EP inhibits TNF secretion by LPS-stimulated RAW 264.7 murine macrophage-like cells [6]. Accordingly, we used inhibition of LPS-induced TNF secretion as one of our screening assays. As depicted in Table 2, each compound was tested at two concentrations (1 or 5 mM) using two different doses of LPS (0.01 or 1.0 μg/ml) for two periods of incubation (12 or 24 h). At the concentrations tested, EP (compound 1), 2AA (compound 10), and DEOP (compound 11) were the most effective inhibitors of LPS-induced TNF production by cultured RAW 264.7 cells (Fig. 1A). At the concentrations tested, many of the screened compounds inhibited LPS-induced $NO^{\bullet}$ production to 40–80% of the control level (Fig. 1B). However, in this assay, the most active compounds were EP

Table 2
Experimental conditions for screening assays using LPS-stimulated RAW 264.7 cells

Condition	Final concentration of LPS (μg/ml)	Final concentration of test compound (mM)	Duration of incubation (h)
1	0.01	1	12
2	1.0	1	12
3	0.01	5	12
4	1.0	5	12
5	0.01	1	24
6	1.0	1	24
7	0.01	5	24
8	1.0	5	24

Table 1
Compounds screened for anti-inflammatory or cytoprotective activities

1Ethyl pyruvate	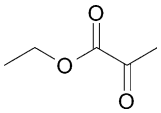	92-Oxopropanal dimethylacetal	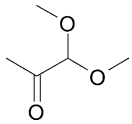
2Ethyl 2-oxo-4-methylpentanoate	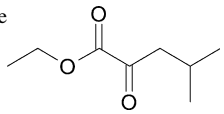	102-Acetamido-acrylic acid	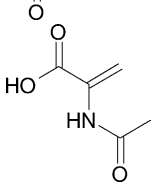
3Ethyl 3-oxobutyrate	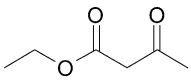	11Diethyl oxalo-proprionate	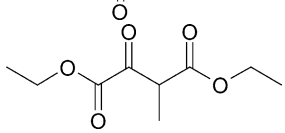
4Diethyl ketomalonate	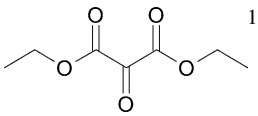	12Dihydroxyacetone dimer	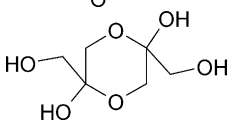
52-Oxobutyric acid	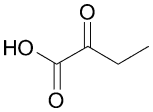	132-Oxosuccinic acid	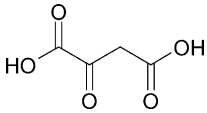
6Ethyl L-lactate	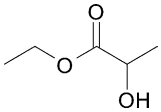	142-Oxoglutaric acid	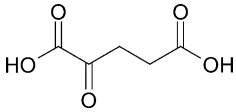
7Ethyl 2,4-dioxopentanoate	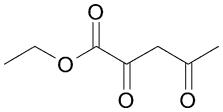	152-Oxo-4-methylglutaric acid	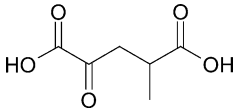
8Ethyl 2-oxo-3-methylbutyrate	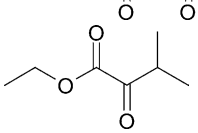	164-Hydroxy-2,2,66-tetramethylpiperidynyl-1-oxy (4-OH TEMPO)	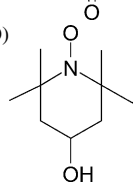

(compound 1), 2AA (compound 10), DEOP (compound 11), and 2-oxosuccinic acid (compound 13).

2.2. EP, 2AA, and DEOP ameliorate the increase in epithelial permeability induced by incubating Caco-2 monolayers with cytomix

When Caco-2 monolayers growing on filters in bicameral diffusion chambers are incubated for 24–48 h with cytomix, the permeability of these model epithelia increases significantly [13]. We previously reported that EP (but not sodium pyruvate) inhibits the development of cytomix-induced hyperpermeability [13]. In the present set of experiments, two compounds, 2AA (compound 10) and DEOP (compound 11), almost completely prevented the development of increased epithelial permeability when Caco-2 monolayers were incubated with cytomix for 48 h (Fig. 2). EP (compound 1) and 2-oxosuccinic acid (compound 13) also markedly inhibited the development of hyperpermeability, although both of these compounds were slightly less active than either 2AA or DEOP.

2.3. 2AA and DEOP inhibit cytomix-induced NF-κB DNA binding

We previously reported that EP inhibits activation of the pro-inflammatory transcription factor, NF-κB, in LPS-stimulated RAW 264.7 cells [6,15] and cytomix-stimulated Caco-2 cells [13]. Because 2AA and DEOP were as or more active than EP in three assay systems (i.e., LPS-induced TNF secretion by RAW 264.7 cells, LPS-induced nitric oxide production by RAW 264.7 cells, and cytomix-induced hyperpermeability of Caco-2 monolayers), we sought to determine whether these compounds inhibit NF-κB DNA binding in immunostimulated cells. As shown in Fig. 3, incubating Caco-2 cells with 1 or 5 mM 2AA (compound 10) completely inhibited cytomix-induced NF-κB DNA binding in nuclear extracts. When Caco-2 cells were incubated with 5 mM DEOP (compound 11), cytomix-induced NF-κB DNA binding was completely inhibited. In contrast, 1 mM DEOP only partially inhibited cytomix-induced NF-κB DNA binding.

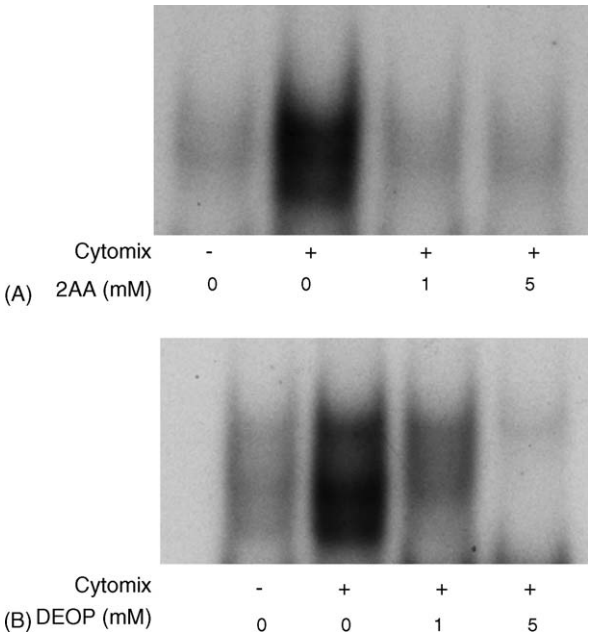

Fig. 3. Effect of 2AA (Panel A) or DEOP (Panel B) on cytomix-induced NF-κB DNA-binding in Caco-2 cells. The cells were incubated in the absence of cytomix or in the presence of cytomix or in the presence of cytomix plus 1 or 5 mM 2AA or DEOP. Nuclear extracts were obtained after 4 h incubation and analyzed for NF-κB DNA binding by EMSA. The results shown are representative of experiments that were repeated at least three times. We previously presented results from supershift and competitive inhibition experiments to document the identity of the protein DNA-complex depicted [13].

2.4. EP, 2AA, and DEOP do not inhibit cytomix-induced IκB degradation but do inhibit translocation of p65 into the nucleus

The activation of NF-κB requires phosphorylation of the IκB subunit by IκB kinase and subsequent proteasomal degradation of IκB [24]. Thus, one way that EP, 2AA, and DEOP might inhibit cytomix-induced NF-κB activation in Caco-2 cells is by blocking one or more of the proximal steps in the activation pathway, and thereby preventing degradation of IκB. In order to test this hypothesis, we assessed the effect of 5 mM EP, 2AA, and DEOP on cytomix-induced degradation of IκBα and IκBβ. In a preliminary time course experiment, we determined that the concentration of IκBα in whole cell extracts was minimal at 30 min after stimulating Caco-2 cells with cytomix (data not shown). Accordingly, this point was evaluated in subsequent experiments. As expected based on previously published work from our laboratory [25], EP had no effect on cytomix-induced degradation of IκBα and IκBβ (Fig. 4). And, consistent with the notion that 2AA and DEOP exert pharmacological effects that are similar to those mediated by EP, neither 2AA nor DEOP affected cytomix-induced degradation of IκBα and IκBβ. Since we previously showed that EP targets a critical cysteine residue involved in DNA binding by p65 [25], we were not

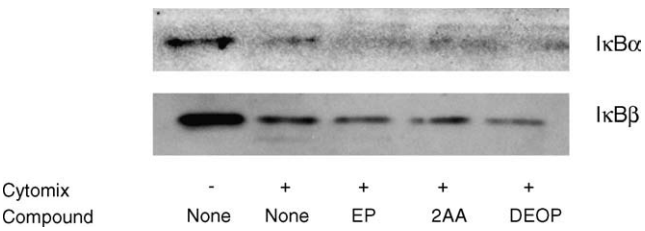

Fig. 4. Effect of 5 mM EP, 2AA or DEOP on IκBα and IκBβ degradation in cytomix-stimulated Caco-2 cells. The cells were incubated with or without cytomix in the presence or absence of the indicated compounds. After incubation for 30 min, whole-cell lysates were prepared, and Western blots were analyzed. The results depicted are representative of an experiment that was repeated twice with similar findings.

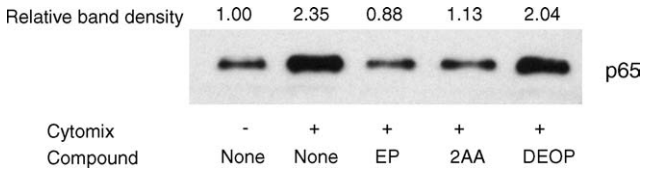

Fig. 5. Effect of 5 mM EP, 2AA or DEOP on translocation of p65 into the nucleus of cytomix-stimulated Caco-2 cells. The cells were incubated with or without cytomix in the presence or absence of the indicated compounds. After incubation for 4 h, nuclear extracts were prepared, and Western blots were analyzed. Densitometry was carried out using Scion Image (release 4.0.3.2). The results depicted are representative of an experiment that was repeated three times with similar findings.

surprised to observe that treating cells with EP inhibited cytomix-induced nuclear translocation of this protein (Fig. 5). 2AA inhibited cytomix-induced nuclear translocation of p65 to about the same extent as EP. DEOP also inhibited nuclear translocation of p65, but to a lesser extent than either EP or 2AA.

2.5. 2AA and DEOP inhibit cytomix-induced iNOS expression

Previously, we reported the EP inhibits cytomix-induced iNOS expression in Caco-2 monolayers [13]. In order to determine if 2AA and DEOP have similar pharmacological effects, Caco-2 cells were incubated for 24 h in the absence or presence of cytomix. In some cases, the cells were co-incubated with cytomix plus 5 mM EP, 2AA or DEOP. As depicted in Fig. 6, all three compounds inhibited the induction of iNOS mRNA expression following incubation of the cells with cytomix.

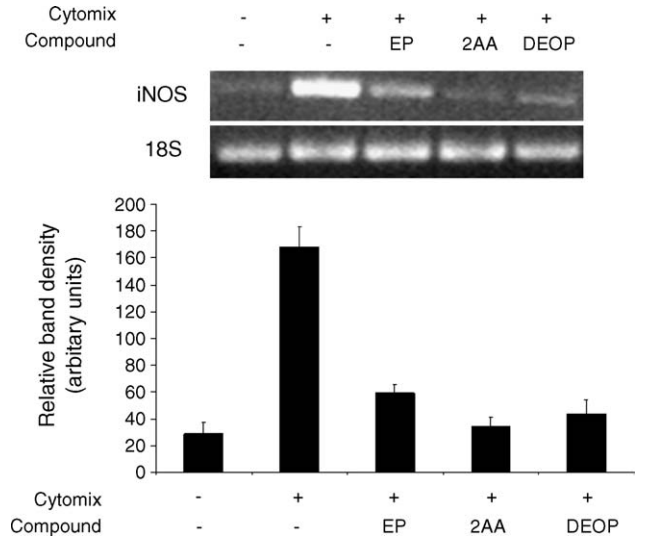

Fig. 6. Effect of EP, 2AA or DEOP on cytomix-induced iNOS mRNA expression in Caco-2 cells. The cells were incubated in the absence of cytomix or in the presence of cytomix or in the presence of cytomix plus 5 mM EP, 2AA or DEOP. Cells were harvested after 24 h incubation and analyzed for iNOS mRNA using semi-quantitative RT-PCR. Densitometry data are means ± S.E.M. ($n = 4$ per condition). Since mRNA was assessed using semi-quantitative RT-PCR, the data were not evaluated statistically.

2.6. Treatment with EP, 2AA or DEOP ameliorates gut barrier dysfunction, attenuates hepatocellular injury, decreases circulating nitrite concentration, and improves survival in endotoxemic mice

We previously reported that delayed treatment with EP ameliorates LPS-induced gut barrier dysfunction and hepatocellular injury in mice [13]. In order to determine if 2AA or DEOP have similar pharmacological effects in this in vivo model system, mice were challenged with LPS and either treated with vehicle or equimolar doses of one of three compounds (EP, 2AA or DEOP). The vehicle or the test compounds all were injected intraperitoneally 1, 6, and 12 h after the injection of LPS. Because we observed efficacy with 0.34 mmol/dose of EP in our prior study [13], we used the same dose for EP, 2AA, and DEOP in the present study in order to provide comparability with our previously published results.

Eighteen hours after the injection of LPS, the mice were sacrificed to obtain blood for the measurement of plasma ALT (a marker of hepatocellular injury). At the same time, a segment of ileum was harvested for determination of mucosal permeability to FD4. Additionally, the MLN complex was harvested for assessing bacterial translocation. One group of mice was not challenged with LPS and served as controls. Treatment with EP, 2AA or DEOP significantly decreased circulating ALT levels 18 h after the induction of endotoxemia (Fig. 7). Similarly, treatment with any of these three compounds significantly ameliorated LPS-induced ileal mucosal hyperpermeability to FD4 (Fig. 8) and bacterial translocation to MLN (Fig. 9). With

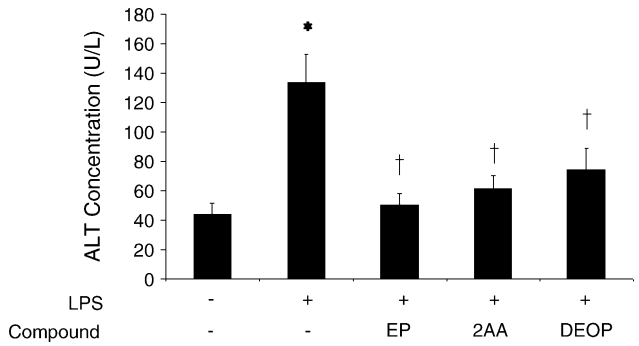

Fig. 7. Effect of treatment with EP, 2AA or DEOP on plasma ALT concentration in endotoxemic mice. Groups of mice ($n = 5$ per condition) were injected with vehicle or 0.1 μg LPS. Some animals were post-treated with three doses of EP, three doses of 2AA or three doses DEOP (0.34 mmol/dose). The compounds were administered 1, 6, and 12 h after the injection of LPS. At 18 h, blood was obtained by cardiac puncture, and plasma collected for subsequent determination of ALT concentration. Results are means ± S.E.M. $^{*}p < 0.05$ vs. the LPS(−) compound(−) control condition. $^{\dagger}p < 0.05$ vs. the LPS(+) compound(−) control condition.

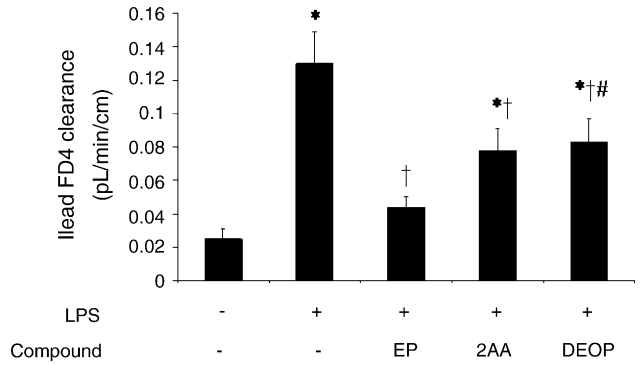

Fig. 8. Effect of treatment with EP, 2AA or DEOP on ileal mucosal permeability in endotoxemic mice. Groups of mice ($n = 5$ per condition) were injected with vehicle or 0.1 μg LPS. Some animals were post-treated with three doses of EP, three doses of 2AA or three doses DEOP (0.34 mmol/dose). The compounds were administered 1, 6, and 12 h after the injection of LPS. At 18 h, the mice were sacrificed and segments of ileum obtained for measurements of mucosal permeability to the hydrophilic macromolecule, FD4. Permeability was assessed using the everted gut sac technique, as described in Section 1. Results are means ± S.E.M. $^{*}p < 0.05$ vs. the LPS(−) compound(−) control condition. $^{\dagger}p < 0.05$ vs. the LPS(+) compound(−) control condition. $^{\#}p < 0.05$ vs. the LPS(+) EP(+) treatment condition.

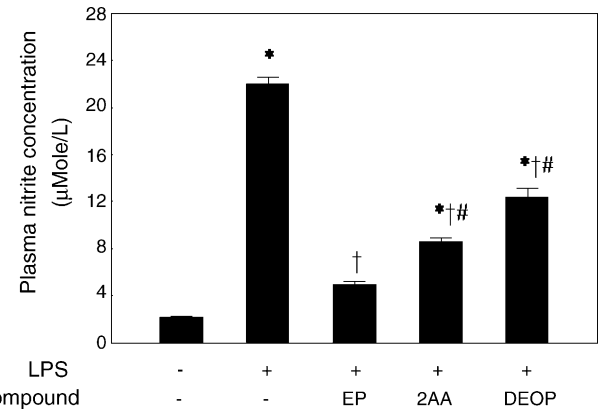

Fig. 10. Effect of treatment with EP, 2AA or DEOP on plasma nitrite concentration in endotoxemic mice. Groups of mice ($n = 5$ per condition) were injected with vehicle or 0.1 μg LPS. Some animals were post-treated with three doses of EP, three doses of 2AA or three doses DEOP (0.34 mmol/dose). The compounds were administered 1, 6, and 12 h after the injection of LPS. At 18 h, blood was obtained by cardiac puncture, and plasma collected for subsequent determination of nitrite concentration. Results are means ± S.E.M. $^{*}p < 0.05$ vs. the LPS(−) compound(−) control condition. $^{\dagger}p < 0.05$ vs. the LPS(+) compound(−) control condition. $^{\#}p < 0.05$ vs. the LPS(+) EP(+) treatment condition.

respect to all three of these parameters, EP was somewhat more effective than either 2AA or DEOP.

Previously, we showed that treatment with EP decreases $NO^{\bullet}$ production in endotoxemic mice [14]. Therefore, in the present study, we measured plasma nitrite concentration, an in index of $NO^{\bullet}$ synthesis, 18 h after injection with LPS (or the PBS vehicle). As expected, the circulating nitrite level was significantly increased in endotoxemic mice treated with PBS but not those treated with EP (Fig. 10). Treatment with either 2AA or DEOP also decreased plasma nitrite concentration 18 h after injection of LPS, although both of these compounds were less effective than EP.

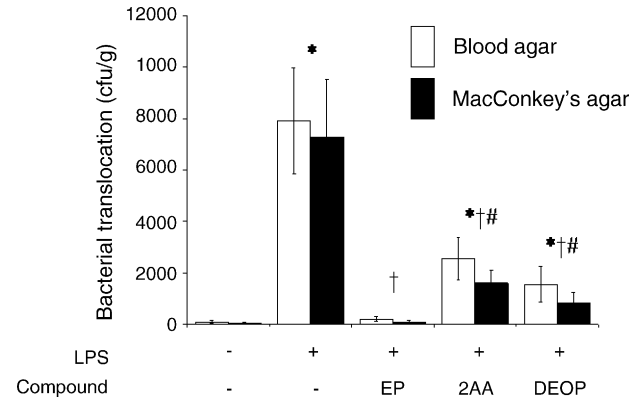

Fig. 9. Effect of treatment with EP, 2AA or DEOP on bacterial translocation to MLN in endotoxemic mice. Groups of mice ($n = 5$ per condition) were injected with vehicle or 0.1 μg LPS. Some animals were post-treated with three doses of EP, three doses of 2AA or three doses DEOP (0.34 mmol/dose). The compounds were administered 1, 6, and 12 h after the injection of LPS. At 18 h, the mice were sacrificed and MLN harvested for determination of bacterial translocation. Samples of tissue homogenates were cultured on blood agar (all aerobic and facultatively anaerobic organisms) and MacConkey's agar (Gram-negative organisms only). Results are means ± S.E.M. $^{*}p < 0.05$ vs. the LPS(−) compound(−) control condition. $^{\dagger}p < 0.05$ vs. the LPS(+) compound(−) control condition. $^{\#}p < 0.05$ vs. the LPS(+) EP(+) treatment condition.

Ulloa et al. reported that pre- or post-treatment with EP significantly improves survival of mice challenged with a lethal dose of LPS [6]. In an effort to determine whether the related compounds, 2AA and DEOP, have similar salutary effects on survival, we injected groups of C57Bl/6 mice with an LD90 dose of LPS and post-treated the animals with equimolar doses of EP, 2AA or DEOP according to the schedule described above. As expected, treatment with EP significantly improved survival from 2 (13.3%) of 15 in vehicle-treated endotoxemic controls to 13 (86.7%) of 15 ($p < 0.05$). Eleven (73.3%) of 15 and 10 (66.7%) of 15 endoxemic mice treated with 2AA or DEOP survived, respectively. Both 2AA and DEOP significantly improved survival relative to the vehicle-treated endotoxemic control group ($p < 0.05$).

2.7. Treatment EP, 2AA or DEOP ameliorates hepatic GSH depletion and lipid peroxidation in endotoxemic mice

Previous studies have shown that acute endotoxemia in rodents is associated with hepatic redox stress, as evidenced by increased concentrations in the liver of MDA [26], a marker of lipid peroxidation, and decreased stores within the liver of the endogenous anti-oxidant, GSH [27]. Because EP has been shown to ameliorate lipid peroxidation in rats subjected to hemorrhagic shock [4] and LPS-stimulated RAW 264.7 cells [15], we sought to determine whether treatment with EP, 2AA or DEOP would modulate hepatic redox stress in endotoxemic mice. We employed

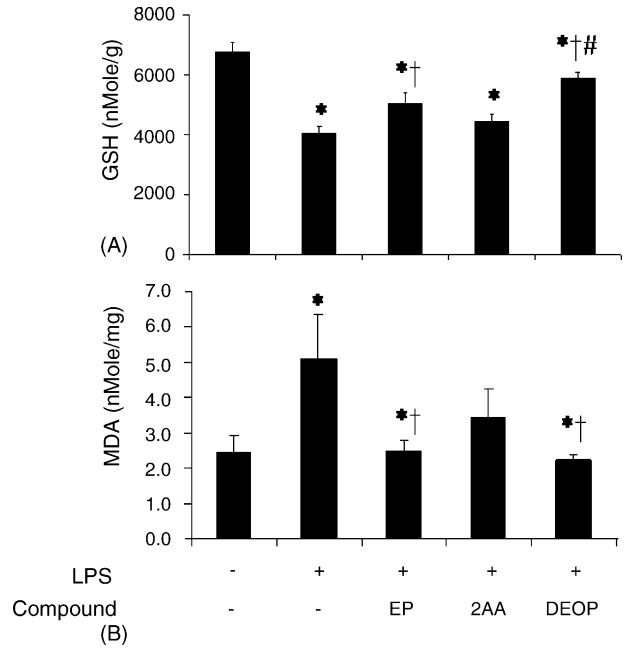

Fig. 11. Effect of treatment with EP, 2AA or DEOP on hepatic GSH content (Panel A) and MDA content (Panel B) in endotoxemic mice. Groups of mice ($n = 5$ per condition) were injected with vehicle or 0.1 μg LPS. Some animals were post-treated with three doses of EP, three doses of 2AA or three doses DEOP (0.34 mmol/dose). The compounds were administered 1, 6, and 12 h after the injection of LPS. At 18 h, liver tissue was obtained for subsequent determination of GSH and MDA levels. Results are means ± S.E.M. $^{*}p < 0.05$ vs. the LPS(−) compound(−) control condition. $^{\dagger}p < 0.05$ vs. the LPS(+) compound(−) control condition. $^{\#}p < 0.05$ vs. the LPS(+) EP(+) treatment condition.

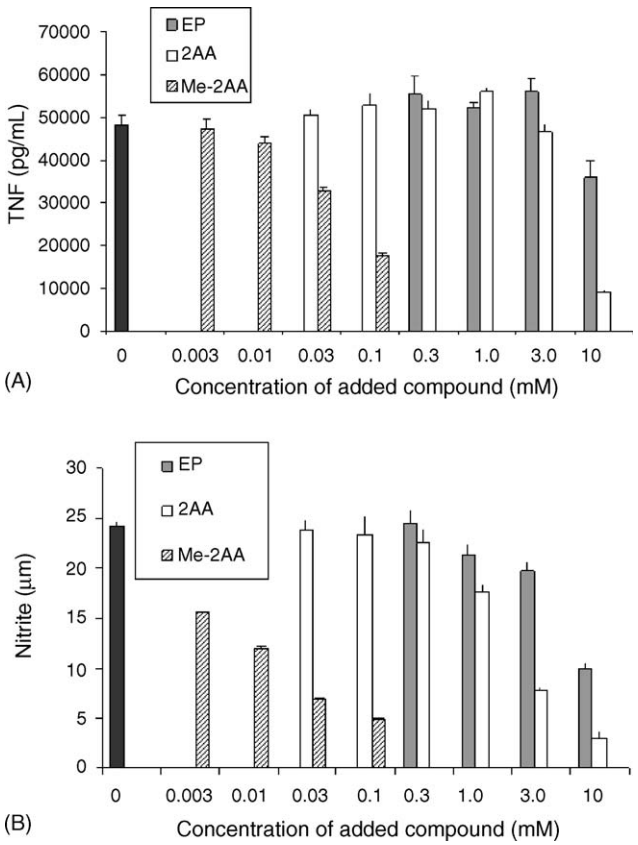

Fig. 12. Effect of graded concentrations of EP, 2AA, and Me-2AA on TNF (Panel A) or $NO^{\bullet}$ (Panel B) release by LPS-stimulated RAW 264.7 cells. The cells were stimulated with LPS (100 ng/ml) for 20 h and supernatants were assayed for TNF by ELISA and nitrite concentration using commercially available kits. Results are means ± S.E.M. ($n = 4$ per condition). In view of the relatively small sample sizes per condition, the data were not evaluated statistically.

the same endotoxemia model and the same treatment schedules as employed for the previous series of experiments. As expected, hepatic GSH content was significantly decreased and hepatic MDA content was significantly increased 18 h after challenging mice with LPS (Fig. 11). Treatment with either EP or DEOP significantly attenuated both of these indices of LPS-induced hepatic redox stress, whereas treatment with 2AA was not effective in this regard.

2.8. Methyl-2-acetamidoacrylate is more potent than 2AA as an anti-inflammatory agent in vitro

We previously reported that the anti-inflammatory effects of EP seem to be mediated, at least in part, by interactions of the compound with key sulfhydryl groups in cells, such as the one in the L-cysteine residue at position 38 (Cys38) of the p65 component of NF-κB [25] or the one in the tripeptide, glutathione (GSH) [15]. Since the ester, methyl-2-acetamidoacrylate, reacts much more rapidly with thiols than does the parent carboxylate [28], we hypothesized that methyl-2-acetamidoacrylate (Me-2AA) might be a more potent anti-inflammatory agent than 2AA. Accordingly, we carried out careful concentration–response studies, evaluating the effects of EP, 2AA, and Me-2AA on TNF (Fig. 12A) and $NO^{\bullet}$ (Fig. 12B) production by LPS-stimulated RAW 264.7 cells. Concentrations of Me-2AA greater than 100 μM were toxic. For both readouts, EP was considerably less potent than either 2AA or Me-2AA. With respect to inhibition of TNF secretion, the apparent EC50 for 2AA was in the range between 3 and 10 mM. In contrast, the apparent EC50 for Me-2AA was in the range between 30 and 100 μM, i.e., Me-2AA was about 100-fold more potent. With regard to inhibition of LPS-induced $NO^{\bullet}$ release, the apparent EC50 for 2AA was between 1 and 3 mM, whereas for Me-2AA it was between 10 and 30 μM. Again, the ester was about 100-fold more potent than the parent carboxylate.

3. Discussion

Although the pharmacological mechanisms that are responsible for the anti-inflammatory effects of EP remain incompletely understood, it is apparent from prior studies that EP is pharmacologically distinct from the closely related compound, sodium pyruvate. Whereas EP inhibits cytomix-induced hyperpermeability of Caco-2 human

enterocyte-like monolayers in a concentration-dependent fashion, equimolar concentrations of sodium pyruvate have no effect in this assay system [13]. Furthermore, in a murine model of LPS-induced gut barrier dysfunction, treatment with EP is significantly more protective than is treatment with equimolar doses of sodium pyruvate, although both compounds provide protection [14]. In another system, mesenteric I/R-induced ileal epithelial injury in rats, EP is clearly more effective on a millimole-for-millimole basis than is sodium pyruvate [1]. Similar findings indicating that EP is more effective than sodium pyruvate were reported by Varma et al., who compared the two compounds in an in vitro study of redox-mediated cellular injury [29].

Given their close chemical similarity, it is remarkable that differential pharmacological effects have been observed when EP and pyruvate have been compared head-to-head in models of inflammation or redox stress. Nevertheless, there are data from studies in a totally unrelated field – the regulation of insulin secretion by pancreatic islet cells – that support the idea that the pharmacological actions of pyruvate esters are quite distinct from those of pyruvate anion. In 1996, Mertz et al. reported that insulin secretion by cultured mouse pancreatic islet cells is stimulated by adding methyl pyruvate but not sodium pyruvate to the culture medium [30]. These investigators further showed that methyl pyruvate – but not sodium pyruvate – causes closure of ATP-sensitive potassium channels, triggers a sustained rise in intracellular calcium ion concentration, and increases insulin secretion more effectively than glucose. Zawalich and Zawalich subsequently showed that methyl pyruvate, but not sodium pyruvate, is a potent insulin secretagogue in freshly isolated rat pancreatic islet cells [31]. The authors of this study speculated that esterification renders pyruvate more membrane-permeable and thereby allows higher levels of the compound to accumulate in mitochondria. This notion is supported by data reported by Malaisse et al., who showed that methyl pyruvate causes less lactate production than sodium pyruvate in pancreatic islets, a finding that is consistent with decreased cytoplasmic metabolism and increased mitochondrial metabolism by the ester [32]. Furthermore, Rocheleau et al. recently reported that the addition of methyl pyruvate (instead of sodium pyruvate) causes a larger and more sustained increase in the cellular content of nicotinamide adenine dinucleotide (NADH) and nicotinamide adenenine dinucleotide phosphate (NADPH) in islet cells [33]. The NADH/NADPH response also occurs faster with methyl pyruvate than is observed with either glucose or sodium pyruvate. These data are consistent with the view that the pyruvate ester stimulates mitochondrial production of both NADPH and NADH. Thus, the differential permeability hypothesis seems likely to be right, at least with respect to the effect of pyruvate esters on insulin secretion. EP probably penetrates through biological membranes more readily than pyruvate because it is more lipophilic. The calculated log *P* for EP is 0.58, whereas the calculated log *P* for pyruvic acid is −0.68.

Originally, we believed that the all of the biological effects of EP, including its actions as an anti-inflammatory agent and its ability to protect against various forms of ischemia/reperfusion-induced tissue injury [1,2,34], were related to two basic mechanisms: ‘‘metabolic support’’ and ‘‘reactive oxygen species (ROS) scavenging’’. The ‘‘metabolic support’’ idea was alluded to above in the discussion about insulin secretion by pancreatic islet cells. Pyruvate is a substrate for the tricarboxylic acid (TCA) cycle in mitochondria, and thus, can promote ATP synthesis within cells. Indeed, some data support the view that pyruvate functions pharmacologically, at least in part, by supporting ATP synthesis [35]. Being more membrane-permeable than pyruvate, EP might be more efficacious than the parent compound from this metabolic standpoint.

The ‘‘ROS scavenging’’ hypothesis derives from the recognition that pyruvate, like other α-keto acids, reacts rapidly and nonenzymatically with H_2O_2 [21,36]. This type of reaction is called oxidative decarboxylation. With pyruvate as a substrate, the reaction yields acetate, carbon dioxide and water. Like pyruvate, EP also rapidly and stoichiometrically scavenges hydrogen peroxide (Englert J.A., Kagan V.E., Fink M.P., unpublished observations). Furthermore, treatment with EP decreases biochemical evidence of oxidant stress in cultured cells [29] and in rodent models of ischemia/reperfusion injury or hemorrhagic shock [4,34].

Results from a key series of experiments suggested to us that neither the ‘‘metabolic support’’ mechanism nor the ‘‘ROS scavenging’’ mechanism was likely to be sufficient (either alone or in combination) to explain the anti-inflammatory effects of EP. In this series of experiments, Sappington et al. showed that transient exposure of Caco-2 monolayers to EP provides durable protection against cytomix-induced hyperpermeability, even when the cells are washed extensively several hours prior to adding the mixture of cytokines [14]. In other words, transient exposure to EP is sufficient to inhibit the response of cells to a subsequent pro-inflammatory stimulus. This observation seems inconsistent with either the ‘‘ROS scavenging’’ or ‘‘metabolic support’’ hypotheses, since to carry out either of these functions, a pharmacological agent would need to be present in the cell during the period of redox or metabolic stress. The durability of the anti-inflammatory effects of EP (even after washing away the compound) suggested to us that EP might covalently modify one or more proteins (or other intracellular constituents), thereby leading to a persistent alteration in the cell’s response to pro-inflammatory cytokines or LPS. This notion gained further support when we showed that treatment with EP targets a critical cysteine residue in the Rel protein, p65, which thereby inhibits DNA binding by the pro-inflammatory transcription factor, NF-κB [25]. In the present study, we further extended this line of investigation by

showing that EP inhibited translocation of p65 into the nucleus following stimulation of Caco-2 cells with cytomix.

Two findings from the present study provide further cause to question the notion that either ''ROS scavenging'' or ''metabolic support'' can fully explain the anti-inflammatory effects of EP. First, 4-OH TEMPO (compound 16), which is known to be an effective cell-permeable ROS scavenger [37–39], was not as active as EP (on a millimole-for-millimole basis) in the three screening assays employed herein to assess anti-inflammatory activity. This observation confirms findings reported by us previously, wherein we showed that another widely studied anti-oxidant, *N*-acetylcysteine, was not as active as EP with respect to inhibition of IL-6 or $NO^{\bullet}$ release by LPS-stimulated RAW 264.7 cells [15]. Second, dihydroxy acetone (compound 12), a simple three-carbon sugar that is converted by cells, including enterocytes, into pyruvate and subsequently used as an oxidative substrate [19,20], also was much less active than EP in the screening assays employed to assess anti-inflammatory activity.

In an effort to gain a better understanding of the mechanism(s) responsible for the pharmacological effects of EP, we screened a series of related compounds for anti-inflammatory activity in vitro. In this screen, two compounds, namely 2AA (compound 10) and DEOP (compound 11) were quite active in all three screens (i.e., suppression of LPS-induced TNF release from RAW 264.7 cells, inhibition of LPS-induced $NO^{\bullet}$ release from RAW 264.7 cells, and inhibition of cytomix-induced hyperpermeability of Caco-2 monolayers). Accordingly, these two compounds were subjected to additional testing, using both in vitro and in vivo assays. Both compounds clearly inhibited cytomix-induced NF-κB DNA binding and iNOS induction in cytomix-stimulated Caco-2 cells. Like EP, neither 2AA nor DEOP inhibited degradation of IκB in cytomix-stimulated Caco-2 cells, suggesting that blockade of the NF-κB signaling by these compounds occurs distal to this step in the signal transduction pathway. Like EP, 2AA, and (to a lesser extent) DEOP inhibited translocation of p65 into the nucleus of cytomix-activated Caco-2 cells. This finding is consistent with the notion that all three of these compounds target DNA binding by the p65 component of the NF-κB complex.

Similarly, both 2AA and DEOP ameliorated LPS-induced hepatocellular injury and gut mucosal barrier dysfunction in mice, even when treatment was started 60 min after injecting the animals with endotoxin. Importantly, both compounds significantly improved the survival of mice challenged with a lethal dose of LPS, despite being administered in a clinically relevant post-treatment fashion.

Whereas DEOP and 2AA both demonstrated anti-inflammatory activity in vitro and diminished LPS-induced organ injury and mortality in vivo, only the former compound significantly ameliorated hepatic redox stress in mice challenged with LPS. Treatment with EP also was associated with better preservation of hepatic GSH content and greater inhibition of hepatic MDA formation in endotoxemic mice. Since EP and DEOP are both α-keto esters, but 2AA is neither an α-keto ester nor an α-keto carboxylate, it is tempting to speculate that this motif is important for protection against LPS-induced redox stress, perhaps because compounds with this structure, as noted above, are capable of scavenging H_2O_2.

We were not too surprised when we observed that DEOP shared some of the pharmacological effects of EP, since both of these compounds are aliphatic α-keto esters. In contrast, we were initially quite surprised to observe that 2AA, which is also called *N*-acetyldehydroalanine, was quite active as an anti-inflammatory agent in both the screening assays and the more extensive in vitro and in vivo tests. Upon further reflection, however, we recognized that EP (Fig. 13A) can enolize, forming the structure shown in Fig. 13B. This same structure is recapitulated by the enol tautomer of DEOP (Fig. 13D) as well as both 2AA (Fig. 13E) and Me-2AA (Fig. 13F). The structural motif shared by all these compounds is the presence a carbon–carbon double bond conjugated to a carbonyl (C=O) group. Many compounds with this general structure are electrophiles that can undergo Michael-type addition reactions with nucleophiles, such as the thiol groups in cysteine residues. It is noteworthy in this regard, that compounds with the general structure, $R\text{-}CH{=}CR'\text{-}\overset{\overset{O}{\|}}{C}\text{-}X$, tend to be more reactive Michael acceptors when X is –OR'' than when X is $-O^{-}$ (i.e., esters are better Michael acceptors than are the corresponding carboxylate anions) [40].

In aqueous solution, the keto–enol equilibrium for pyruvate favors the keto form to a very large extent [41–43]. The rate of enolization, however, is substantial, especially

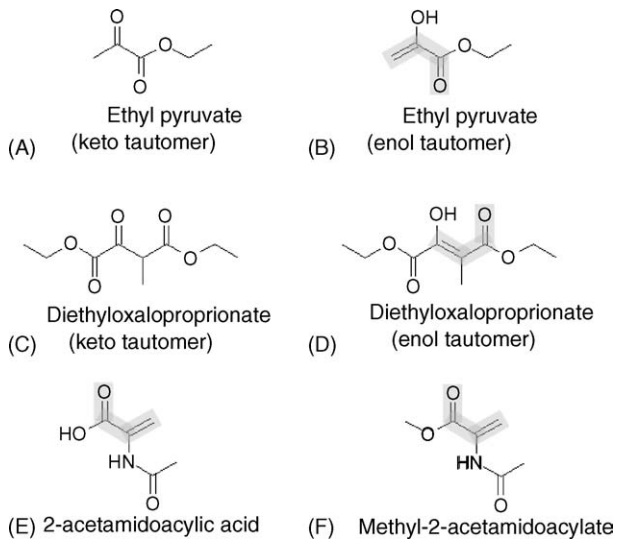

Fig. 13. Chemical structures of keto and enol forms of EP (Panels A and B, respectively) and DEOP (Panels C and D, respectively) as well as 2AA (Panel E) and Me-2AA (Panel F). Shaded areas highlight the conjugated olefin–carboxyl structure that is shared by the indicated compounds.

in the presence of a divalent cation, such as ionized calcium or magnesium [44,45]. Thus, it is conceivable that some of the pharmacological effects of EP are actually mediated by the enol tautomer. DEOP, like EP, is an α-keto ester. But, because it has a 1,3-dicarbonyl structure, internal hydrogen bonding and resonance greatly stabilize the enol form; indeed, for many compounds with this structure (e.g., 2,4-pentanedione), the enol form predominates in aqueous solution. Three other compounds, namely ethyl 3-oxobutyrate (compound 3), ethyl 2,4-dioxopentanoate (compound 7), and 2-oxosuccinic acid (compound 13) also incorporate the 1,3-dicarbonyl motif, and might be expected to enolize extensively. Interestingly, all three of these compounds showed at least some anti-inflammatory activity in the three screening assays employed in this study.

As noted above, EP is pharmacologically more active than pyruvate in various in vitro and in vivo assay systems [1,13,14]. Since 2AA is a carboxylate, we wondered whether an ester derived from this compound would manifest the same tendency toward greater anti-inflammatory activity relative to the parent carboxylate. Indeed, when we carried out careful concentration–response studies, comparing 2AA and Me-2AA, the ester was approximately 100-fold more potent than the parent compound. By the same token, however, Me-2AA was also clearly toxic to RAW 264.7 cells at concentrations greater than 100 μM, whereas 2AA and EP were apparently devoid of toxic effects, even at concentrations as high as 10 mM.

Potent electrophiles, of course, are often toxic to cells, because of their tendency to covalently modify nucleic acids and proteins and deplete GSH (thereby increasing cellular susceptibility to redox stress). The remarkable salutary effects of EP in a variety of in vivo systems [1,5,6,8,10–13] may reflect a fortuitous combination of its relatively low (but not absent) reactivity as an electrophile (and, therefore, low toxicity) combined with its ability to act as an H_2O_2 scavenger (and, therefore, ameliorate redox stress) and serve as a metabolic substrate (and, therefore, reduce ATP depletion and/or mitochondrial damage). In other words, EP, which is not found normally in cells, improves on mother nature's compound, pyruvate, as a pharmacological agent; but, efforts to improve upon the pyruvate motif still further may not be successful, because increased anti-inflammatory potency may go hand in hand with increased toxicity.

Reference

[1] Sims CA, Wattanasirichaigoon S, Menconi MJ, Ajami AM, Fink MP. Ringer's ethyl pyruvate solution ameliorates ischemia/reperfusion-induced intestinal mucosal injury in rats. Crit Care Med 2001;29:1513–8.

[2] Uchiyama T, Delude RL, Fink MP. Dose-dependent effects of ethyl pyruvate in mice subjected to mesenteric ischemia and reperfusion. Intensive Care Med 2003;29:2050–8.

[3] Woo YJ, Taylor MD, Cohen JE, Jayasankar V, Bish LT, Burdick J, et al. Ethyl pyruvate preserves cardiac function and attenuates infarct size following prolonged myocardial ischemia. J Thorac Cardiovasc Surg 2004;127:1262–9.

[4] Tawadrous ZS, Delude RL, Fink MP. Resuscitation from hemorrhagic shock with Ringer's ethyl pyruvate solution improves survival and ameliorates intestinal mucosal hyperpermeability in rats. Shock 2002;17:473–7.

[5] Yang R, Gallo DJ, Baust JJ, Uchiyama T, Watkins SK, Delude RL, et al. Ethyl pyruvate modulates inflammatory gene expression in mice subjected to hemorrhagic shock. Am J Physiol Gastrointest Liver Physiol 2002;283:G212–22.

[6] Ulloa L, Ochani M, Yang H, Halperin D, Yang R, Czura CJ, et al. Ethyl pyruvate prevents lethality in mice with established lethal sepsis and systemic inflammation. Proc Natl Acad Sci USA 2002;99:12351–6.

[7] Venkataraman R, Kellum JA, Song M, Fink MP. Resuscitation with Ringer's ethyl pyruvate solution prolongs survival and modulates plasma cytokine and nitrite/nitrate concentrations in a rat model of lipopolysaccharide-induced shock. Shock 2002;18:507–12.

[8] Miyaji T, Hu X, Yuen PST, Muramatsu Y, Iyer S, Hewitt SM, et al. Ethyl pyruvate decreases sepsis-induced acute renal failure and multiple organ damage in aged mice. Kidney Int 2003;64:1620–31.

[9] Dear JW, Kobayashi H, Jo SK, Holly MK, Hu X, Yuen PS, et al. Dendrimer-enhanced MRI as a diagnostic and prognostic biomarker of sepsis-induced acute renal failure in aged mice. Kidney Int 2005;67:2159–67.

[10] Yang R, Uchiyama T, Alber SM, Han X, Watkins SK, Delude RL, et al. Ethyl pyruvate ameliorates distant organ injury in a murine model of acute necrotizing pancreatitis. Crit Care Med 2004;32:1453–9.

[11] Yang R, Han X, Delude RL, Fink MP. Ethyl pyruvate ameliorates acute alcohol-induced liver injury and inflammation in mice. J Lab Clin Med 2003;142:322–31.

[12] Yang R, Uchiyama T, Watkins SK, Han X, Fink MP. Ethyl pyruvate reduces liver injury in a murine model of extrahepatic cholestasis. Shock 2004;22:369–75.

[13] Sappington PL, Han X, Yang R, Delude RL, Fink MP. Ethyl pyruvate ameliorates intestinal epithelial barrier dysfunction in endotoxemic mice and immunostimulated Caco-2 enterocytic monolayers. J Pharmacol Exp Ther 2003;304:464–76.

[14] Sappington PL, Fink ME, Yang R, Delude RL, Fink MP. Ethyl pyruvate provides durable protection against inflammation-induced intestinal epithelial barrier dysfunction. Shock 2003;20:521–8.

[15] Song M, Kellum JA, Kaldas H, Fink MP. Evidence that glutathione depletion is a mechanism responsible for the anti-inflammatory effects of ethyl pyruvate in cultured LPS-stimulated RAW 264.7 cells. J Pharmacol Exp Ther 2004;308:307–16.

[16] Menconi MJ, Salzman AL, Unno N, Ezzell RM, Casey DM, Brown DA, et al. Acidosis induces hyperpermeability in Caco-2_{BBe} cultured intestinal epithelial monolayers. Am J Physiol 1997;272: G1007–21.

[17] Unno N, Wang H, Menconi MJ, Tytgat SHAJ, Larkin V, Smith M, et al. Inhibition of inducible nitric oxide synthase ameliorates lipopolysaccharide-induced gut mucosal barrier dysfunction in rats. Gastroenterology 1997;113:1246–57.

[18] Langmuir ME, Yang J-R, LeCompte KA, Durand RE. New thiol acitve fluorophores for intracellular thiols and glutathione measurement. In: Slavik J, editor. Fluorescence microscopy and fluorescent probes. New York: Plenum; 1996. p. 229–34.

[19] Ichai C, El-Mir MY, Nogueira V, Piquet MA, Chauvin C, Fontaine E, et al. Exogenous Mg-ATP induces a large inhibition of pyruvate kinase in intact rat hepatocytes. J Biol Chem 2001;276:6398–403.

[20] Vidal H, Comte B, Beylot M, Riou JP. Inhibition of glucose oxidation by vasoactive intestinal peptide in isolated rat enterocytes. J Biol Chem 1988;263:9206–11.

[21] Bunton CA. Oxidation of α-diketones and α-keto-acids by hydrogen peroxide. Nature 1949;163:144.

[22] O'Donnell-Tormey J, Nathan CF, Lanks K, DeBois CJ, de la Harpe J. Secretion of pyruvate. An antioxidant defense of mammalian cells. J Exp Med 1987;165:500–14.
[23] Dobsak P, Courdertot-Masuyer C, Zeller M, Vergely C, Laubriet A, Assem M, et al. Antioxidative properties of pyruvate and protection of the ischemic rat heart during cardioplegia. J Cardiovasc Pharmacol 1999;34:651–9.
[24] Senftleben U, Karin M. The IKK/NF-κB pathway. Crit Care Med 2002;30:S18–26.
[25] Han Y, Englert JA, Yang R, Delude RL, Fink MP. Ethyl pyruvate inhibits NF-{kappa}B-dependent signaling by directly targeting p65. J Pharmacol Exp Ther 2005;312:1097–115.
[26] Zhang C, Walker LM, Hinson JA, Mayeux PR. Oxidant stress in rat liver after lipopolysaccharide administration: effect of inducible nitric-oxide synthase inhibition. J Pharmacol Exp Ther 2000;293:968–72.
[27] Kang KW, Pak YM, Kim ND. Diethylmaleate and buthionine sulfoximine, glutathione-depleting agents, differentially inhibit expression of inducible nitric oxide synthase in endotoxemic mice. Nitric Oxide 1999;3:265–71.
[28] Snow JT, Finley JW, Friedman M. Relative reactivities of sulfhydryl groups with *N*-acetyl dehydroalanine and *N*-acetyl dehydroalanine methyl ester. Int J Pept Protein Res 1976;8:57–64.
[29] Varma SD, Devamanoharan PS, Ali AH. Prevention of intracellular oxidative stress to lens by pyruvate and its ester. Free Radic Res 1998;28:131–5.
[30] Mertz RJ, Worley JFI, Spencer B, Johnson JH, Dukes ID. Activation of stimulus-secretion coupling in pancreatic β-cells by specific products of glucose metabolism. J Biol Chem 1996;271:4838–45.
[31] Zawalich WS, Zawalich KC. Influence of pyruvic acid methyl ester on rat pancreatic islets. Effects on insulin secretion, phosphoinositide hydrolysis, and sensitization of the beta cell. J Biol Chem 1997;272:3527–31.
[32] Malaisse WJ, Jijakli H, Ulusoy S, Cook L, Best L, Vinambres C, et al. Insulinotropic action of methyl pyruvate: secretory, cationic, and biosynthetic aspects. Arch Biochem Biophys 1996;335: 229–44.
[33] Rocheleau JV, Head WS, Piston DW. Quantitative NAD(P)H/flavoprotein autofluorescence imaging reveals metabolic mechanisms of pancreatic islet pyruvate response. J Biol Chem 2004;279:31780–7.
[34] Tsung A, Kaizu T, Nakao A, Shao L, Bucher B, Fink MP, et al. Ethyl pyruvate ameliorates liver ischemia-reperfusion injury by decreasing hepatic necrosis and apoptosis. Transplantation 2005;27:196–204.
[35] Mallet RT, Sun J. Mitochondrial metabolism of pyruvate is required for its enhancement of cardiac function and energetics. Cardiovasc Res 1999;42:149–61.
[36] Holleman MAF. Notice sur l'action de l'eau oxygénée sur les acétoniques et sur le dicétones 1.2. Recl Trav Chim Pays-bas Belg 1904;23:169–71.
[37] Krishna MC, Russo A, Mitchell JB, Goldstein S, Dafni H, Samuni A. Do nitroxide antioxidants act as scavengers of $O_2^{\bullet -}$ or as SOD mimics? J Biol Chem 1996;271:26026–31.
[38] Hahn SM, Mitchell JB, Shacter E. Tempol inhibits neutrophil and hydrogen peroxide-mediated DNA damage. Free Radic Biol Med 1997;23:879–84.
[39] Mota-Filipe H, McDonald MC, Cuzzocrea S, Thiemermann C. A membrane-permeable radical scavenger reduces the organ injury in hemorrhagic shock. Shock 1999;12:255–61.
[40] Talalay P, De Long MJ, Prochaska HJ. Identification of a common chemical signal regulating the induction of enzymes that protect against chemical carcinogenesis. Proc Natl Acad Sci USA 1988;85:8261–5.
[41] Keeffe JR, Kresge AJ, Schepp NP. Keto–enol equilibrium constants of simple monofunctional aldehydes and ketones in aqueous solution. J Am Chem Soc 1990;112:4862–8.
[42] Chiang Y, Kresge AJ, Pruszynski P. Keto–enol equilibria in the pyruvic acid system: determination of the keto–enol equilibrium constants of pyruvic acid and pyruvate anion and the acidity constant of pyruvate enol in aqueous solution. J Am Chem Soc 1992;114:3103–7.
[43] Esposito A, Lukas A, Meany JE, Pocker Y. The reversible enolization and hydration of pyruvate: possible roles of keto, enol, and hydrated pyruvate in lactate dehydrogenase catalysis. Can J Chem 1999;77:1108–17.
[44] Kosicki GW. Oxaloacetate decarboxylase from cod. Catalysis of hydrogen–deuterium exchange in pyruvate. Biochemistry 1968;7: 4310–4.
[45] Wilton DC. The mechanism of adduct formation between NAD^+ and pyruvate bound to pig heart lactate dehydrogenase. Biochem J 1979;177:951–7.